Proceedings of the International Gas Turbine Congress 2003 Tokyo
November 2-7, 2003

IGTC2003Tokyo TS-012

Interface Construction for Thermal Stress Analysis in Virtual Turbine and Its Application

Jinxiang CHEN, Akinori OGAWA, Ryosaku HASHIMOTO and Toyoaki YOSHIDA
Aeronautical Environment Technology Center, Institute of Space Technology and Aeronautics, Japan Aerospace Exploration Agency
7-44-1 Jindaiji, Chofu, Tokyo 182-8522, JAPAN
Phone: +81-422-40-3475, FAX: +81-422-40-3440, E-mail: chen.jinxiang@jaxa.jp

ABSTRACT

In order to establish the process of structural strength analysis and evaluation of turbine vanes and blades of single crystal Ni-base superalloys for TIT 1700℃ level, an interface that applies the data of CFD and heat transfer analysis to structural strength analysis has been constructed. Thermal stress analysis has been performed by utilizing the interface for turbine vanes of TIT 1400℃ level as a reference condition. As the results, (1) The interpolate process of three dimensions can be disassembled into two steps, selection of that interpolation plane and interpolation in two-dimensional plane. Validity of the constructed interface was verified. (2) The maximum Von Mises stress was situated in the fillet between the trailing edge of pressure side and the outer sidewall of vane. It is clear that stress concentration is easy to take place in the small radius in the relevant region. (3) The visualization method introduced in the present work was very effective for the evaluation of characteristics of thermal stress.

INTRODUCTION

When the turbine inlet temperature (TIT) is higher, thermal efficiency of gas turbines becomes higher, and this is effective to decrease CO2 emission and prevent the globe warming. For this reason, researches of high temperature gas turbines have been done very actively. The "High temperature materials 21 project" is carried out under this background. In this project, research and development of new materials have been conducted on Pt group metals base refractory superalloys for TIT of 1800℃ level, single crystal (SC) Ni-base superalloys for TIT of 1700℃ level and silicon nitride ceramics for TIT of 1500℃ level with no air cooling. Usually, it is required to conduct practical engine verification tests for newly developed materials, however these tests take long time and great cost. Thus only a trial execution of engine verification tests was done for a Ni-base superalloy TMS-82+ in this project. In order to evaluate advantages of new materials when those are applied in gas turbines, a virtual turbine consisted of program packages has been constructed in the project. JAXA (Yoshida et al., 2001) has been engaged in the development of database for the virtual turbine that provides detailed information on aerodynamics, heat transfer and structural strength performance of the high temperature turbine section. As a part of this work, in order to establish the process of structural strength analysis of turbine vanes and blades, the interface which applies the data of CFD and heat transfer analysis (CFD) to structural strength analysis has been constructed and thermal stress analysis has been performed by utilizing the interface. This paper describes the construction of the interface and its applications to turbine vanes of TIT 1400℃ level as a reference condition. The advantages of vanes with film cooling and only with convection cooling are also discussed.

MODEL AND ANALYTICAL CONDITION

Fig. 1 shows the turbine vane model. It is the basis of the supposed form of the virtual turbine in this project. The material is

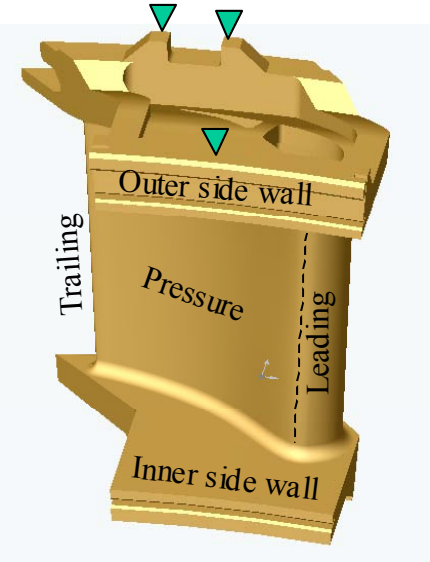

Fig. 1 Turbine vanes model

Manuscript Received on April 24, 2003

the 3rd generation SC Ni-base superalloys TMS-75. This alloy is cubic crystal. When the X, Y, and Z axes are identical with the crystal axes, there are only three independence elastic constants c11, c12 and c44 (Miyazaki and Shiozaki, 1996). Thermal conductivity K , specific heat Cp and thermal expansion coefficient γ are not anisotropy in each direction except elastic coefficients. Therefore the average values obtained by analysis of experiment data are used for all directions.

The CFD data of this project includes two sets of data obtained in two different thermal environments, the convection and the film cooling. Fig. 2 shows the distribution of the CFD data. The interface proposed in this paper reads these temperature data as the thermal load. The outside surface of outer and inner sidewalls was restraint. The analysis is carried out on analysis software NASTRAN for Windows Visual 2002.

INTERFACE CONSTRUCTION, ANALYTICAL RESULTS AND ITS DISCUSSION

INTERFACE CONSTRUCTION

The thermal environment on the pressure and suction surface (Fig. 2) had been described with the form of (X, Y, Z, Tc), in which (X, Y, Z) and Tc denote the coordinate position and the temperature of the mesh nodes, respectively. The strength analysis model in this paper has the same three-dimension pressure and suction surface as the CFD data. Each node in the strength analysis model has five properties, the nodes number, the coordinate position, and the temperature with the form (ID, X, Y, Z, Tx). The temperature Tx must be obtained from the CFD data. However, the strength analysis software has different node numbers and different distribution with CFD data. Then, an interface is needed to convert the temperature Tc of the CFD to the strength analysis model. In this paper, a data conversion method is proposed as following.

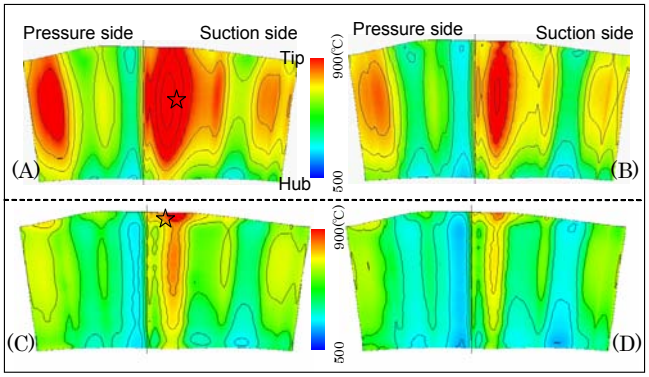

Fig. 2 Metal surface temperature in outside (A, B) and inside (B, D). (A)~(B) , convection, (C) ~(D) , film cooling.

This method converts data with the interpolation of quasi-three dimensions by comparing the spatial coordinates of each node in the strength analytical model with that of CFD nodes and finding adjoining nodes in CFD nodes. For a node E of the strength analysis model (IDe, Xe, Ye, Ze, Te), Fig. 3 explains the proposed conversion method. The Fig. 3 (A) is the external contour of pressure and suction surface of a turbine vane; the Fig. 3 (B) displays the method of detecting the adjoining CFD nodes (● arrow) to the node E (☆ arrow).

After careful analysis of shape of the external pressure and suction surface, it is found that curvature of the contour curve in XY plane is large (as Fig. 3 (A)) and vertical (Z) direction is very flat instead (as Fig. 1). Therefore, the interpolate process of three dimensions can be disassembled into two steps, selection of the interpolation plane between XZ or YZ planes and two-dimensional interpolation on the selected plane. **Selection of interpolation plane**: Projecting the small curved surface around node E to the XZ and YZ plane and chose the plane with larger projected area. This selection is based on the idea that interpolation can be carried out more precisely in larger size area. As an example shown in Fig. 3 (A), the small curve E1 around node E is projected to X and Y as rectilinear E1x and E1y, respectively. E1x is longer than E1y, and it means the curved surface area projected to XZ plan is larger than that of YZ plane. So, it is reasonable to choose XZ plane to be the

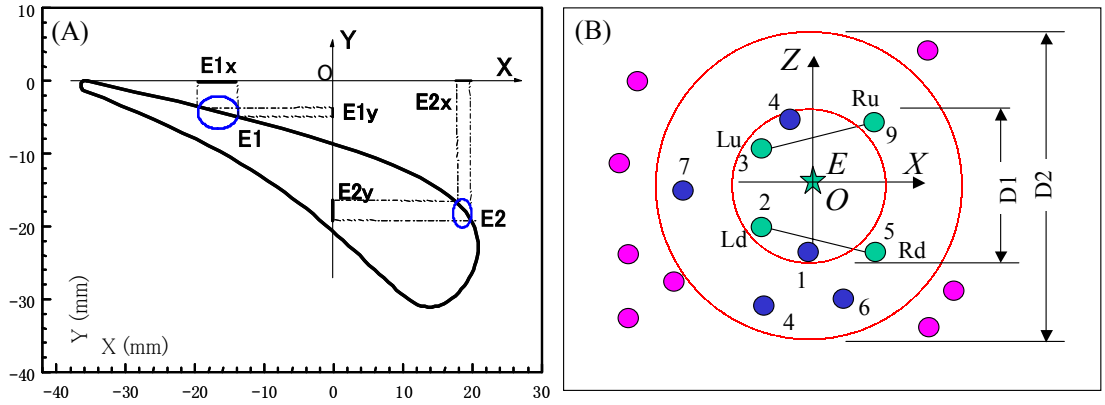

Fig. 3 Interface construction method. (A) selection interpolation plane, (B) detection of CFD nodes.

interpolation plane. Conversely, when node E is situated in the curve E2 (Fig. 3 (A)) where E2y is longer than E2x, YZ plane is selected as the interpolation plane.

Two-dimensional interpolation: After the interpolation plane is decided, node E is set as coordinates origin O, and for four quadrants we detect one CFD node whose spatial distance to origin O is the closest in its quadrant (adjoining nodes). In detail, given an initial diameter D1, four CFD nodes (the number 1~4 CFD nodes) situated in the circle area are found (Fig. 3 (B)). But only the node 3 of the 2nd quadrant and the node 2 of 3rd quadrant are regarded as legal adjoining nodes, no adjoining node can be found in 1st quadrant and 4th quadrant. Then the searching diameter is expanded to the D2 as the adjoining of the 1st and the 4th quadrant (the nodes 9 and 5 respectively) to be taken as adjacent nodes. This process continues until four adjoining nodes are successfully found or the diameter reaches some unreasonable limit (In the case of nodes situated on edges, only two or three adjoining nodes can be found). Then, interpolation of node E can be carried out in two-dimension by the method mentioned as following.

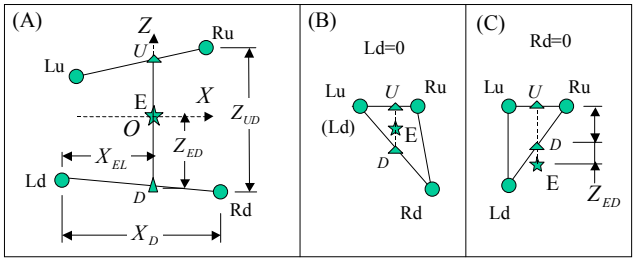

Fig. 4 Interpolation method for four points (A) and three points ((B), (C)).

Fig. 4 (A) shows an example of interpolation in XZ plane. The spatial distribution of node E and the adjoining node is illustrated. Four adjacent nodes are the Ld (the Left and the down), the Ru (the Right and the upper), the Rd and the Ld, respectively. Interpolation point D is the intersection point of the line X = Xe of the present node E and the line connecting the adjacent nodes Ld and Rd. Thus, the Z coordinate Z_D and the temperature T_D of this interpolation point D are decided from the alignment interpolation for the coordinate X axis. In this example, the temperature T_D is obtained by Equation (1) where T_{LD} is the temperature of node Ld and T_{RD} is the temperature of node Rd.

$$T_D = T_{LD} \cdot (1 - \eta_D) + T_{RD} \cdot \eta_D \qquad \cdots\cdots \qquad (1)$$

In this equation, $\eta_D = X_{EL} / X_D$, where X_{EL} and X_D are relative distant shown in Fig. 4 (A) .

The Z coordinate Z_U and the temperature T_U of point U in the Fig. 4 (A) can be gotten by the same method. Then, the temperature T_E of node E is calculated by alignment interpolation of point D and U along the Z-axis.

By the two-step interpolation method, temperature data of each node in strength analysis model can be successful gotten from adjoining nodes. Although the interpolation is executed in two-dimension, we can get enough accurate results with the consideration of three-dimensional distribution of CFD nodes. We call the method a "quasi-three dimensional interpolation ".

But there are also some exceptions that only 3 adjoining nodes or lesser can be found around node E when node E is situated at the

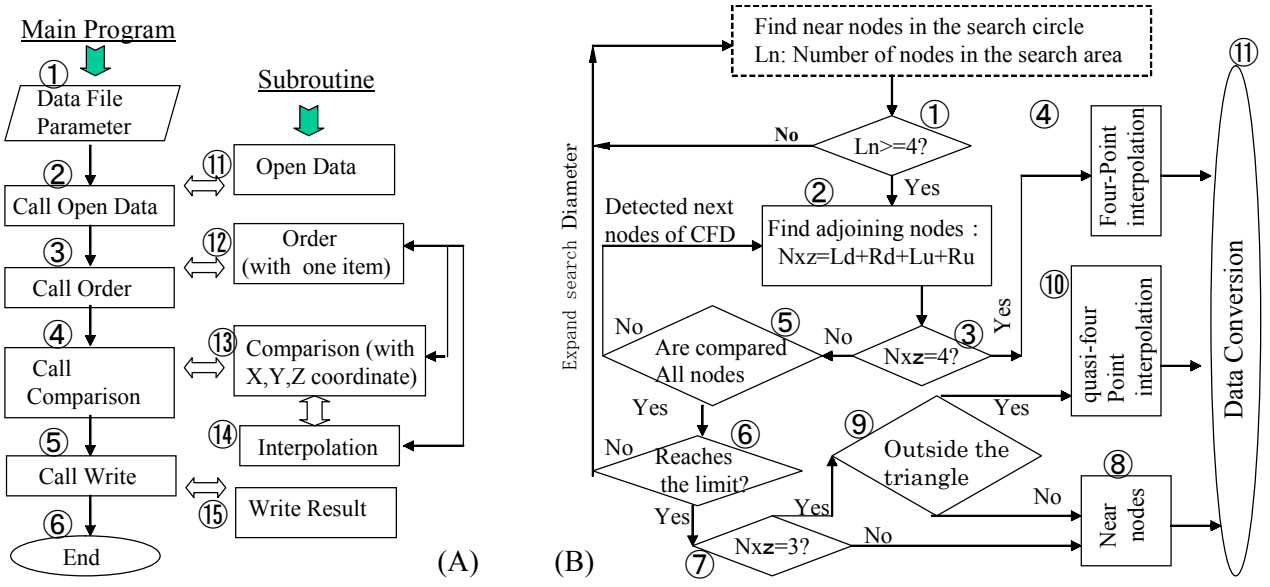

Fig. 5 Interface flow chart for main program (A) and interpolation subroutine (B)

edge of the model. In case of 3 nodes, it is supposed that the adjoining nodes Ld and Lu are piled up as the Fig. 4 (B), the interpolation can also be carried out as normal. When node E is situated outside triangle, (Fig. 3 (C)), the temperature value is obtained by extrapolation (Equation (1)). As the extrapolation precondition, present node E is required to be close to triangle (Fig. 4 (C): $Z_{ED}/Z_{UD} < 1$).

In the following text, we describe the realization of this method and flow chart of the proposed interface in detail. Fig. 5 (A) shows the flow charts of the main program and the interpolation/ extrapolation subroutine. As shown in Fig. 5 (A), parameters such as the number nodes of mesh are inputted in main program ①. The input file data are opened and read in main ② subroutine ⑪(open data). The output data file are opened and written in main ⑤ subroutine ⑮ (write Result). Relative data (e.g. distance between adjoining nodes and present node E) are sorted in main ③, subroutine ⑫ (Order). The determination of interpolation plane, the detection of the adjoining nodes, and interpolation are completed in the main④, Subroutine ⑬(Comparison) and ⑭ (Interpolation). The flow chart of the subroutine Interpolation is shown in Fig. 5 (B). The number of the CFD nodes which are situated in the checked reign (checked nodes) by the subroutine Comparison in Fig. 5 (A) is defined as Ln in Fig. 5 (B) ①. Number of adjoining nodes is denoted as ②Nxz (=Ld+Rd+Lu+Ru) where Ld, Rd, Lu and Ru is set to 1 if an adjoining node is found in the correspondent quadrant and 0 otherwise. If not all four adjoining nodes are found (Nxz < 4) ⑤ and the number Ln of checked nodes were insufficient ⑥, then the search diameter D is expanded. This procedure continues until Ln becomes enough large or Nxz>=4. In the case where Ln is enough large and Nxz is still lower than 4, it is decided that node E is situated on the edge of the model. When adjacent nodes and the number of adjoining nodes were decided, interpolation can be carried out as ④ or ⑧ or ⑩ regard as different condition. For example, ④ is executed if four adjoining nodes are found and ⑧ is executed if there are 3 adjoining nodes. By this algorithm, the interface converts the CFD data to the format which strength analysis can directly use.

As verification, we read external pressure surface CFD data in turbine vanes with the interface proposed. The result is shown Fig. 6 (A) where the broken line displays the leading edge position. Comparing the result in Fig. 6 (A) with Fig. 2 (A, the left side part) at the star point and other points, it is shown that the result in Fig. 6 is accurate.

ANALYTICAL RESULT AND DISCUSSION OF HEAT TRANSFER

The three-dimensional temperature distribution is shown Fig. 6 (B) (C). The lowest temperature point is marked with the ↓ arrows and the high temperature points are marked with the ▲, ☆. The highest temperature is 1028 ℃ and the point is located around ☆ , external suction surface of turbine vanes for the convection (Fig. 6 (A) (B)). Fig. 7 shows the film cooling efficiency. Comparing the film cooling (Fig. 6 (C)) with convection (Fig. 6 (B)), the temperature of the whole turbine vanes goes down substantially because of the high cooling efficiency of film cooling. It is also observed that the temperature distribution becomes rather uniform. Table 1 lists statistic data of temperature for the pressure and suction of turbine vanes. In comparison with that of the convection, the highest temperature of film cooling decreases about

.

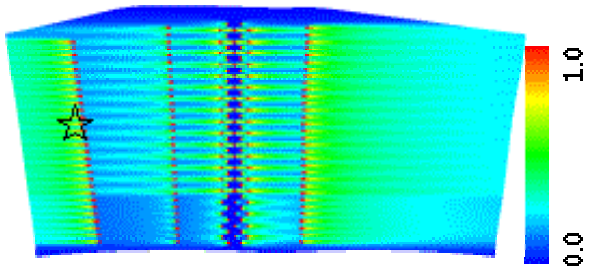

Fig. 7 Film Cooling efficiency

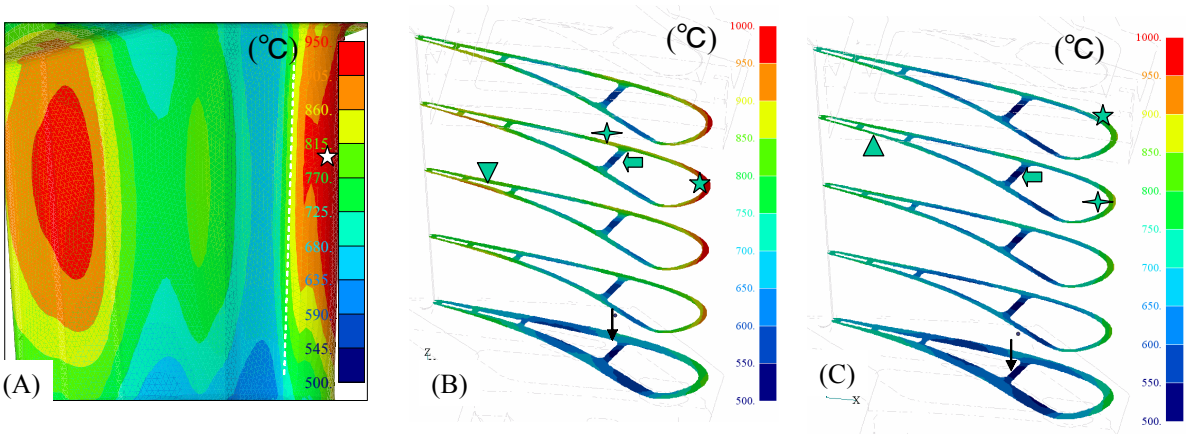

Fig. 6 Temperature distribution: (A) in pressure surface, (B) section of convection, (C) film cooling

90 ℃, the average temperature decreases with similar value, the standard deviation (SD) of temperature goes down 1/3.

Table 1 Temperature statistical characters (℃)

Parameters	Average	Min	Max	SD
Convection	786.8	538.7	1027.8	85.9
Film cooling	702.8	524.5	930.8	59.3

ANALYTICAL RESULT AND DISUSSION OF THERMAL STRESS

Fig. 8 (A) (B) compares Von Mises stress of the convection and film cooling. The maximum thermal stress was situated the topper trailing edge (Fig. 8 ☆) for both cases. Beside this, high Von Mises stress was observed (Fig. 8, ▲, ⇐) around the places where high or low temperature occur (Fig. 6 (B) (C) arrows , ⇐, ↓). Because temperature variation is fierce around these places, namely the temperature gradient is large, thermal stress becomes large. Fig. 8 (C) shows a contour picture around the maximum stress point which is situated in the fillet between the trailing edge of pressure side and the outer sidewall of vane for convection. This may due to the small radius in the relevant region in which stress concentration is easy to take place.

STRESS EVALUTION

Stress evaluation is carried out by using the Von Mises stress normalized by 0.2% proof stress (proof ratio) of its metal temperature as evaluation index.

Proof ratio of each node in pressure and suction of the turbine vanes is calculated and result is shown in the Fig. 9 (A) , (B) . This figure of proof ratio is visualized by utilizing the analysis software. The temperature of the pressure and suction of turbine vanes lies between 525 ℃ and 1028 ℃. But maximum 0.2% proof stress is among the 650 ℃~ 850 ℃. At the marked places where the Von Mises stress is high relatively (Fig. 8 (A) ,⇐, ▲), their correspondent proof stress is relatively low because of the lower or high temperature of these places (Fig. 6 (A)), so the proof ratios (Fig. 9 (A), ⇐, ▲) become high.

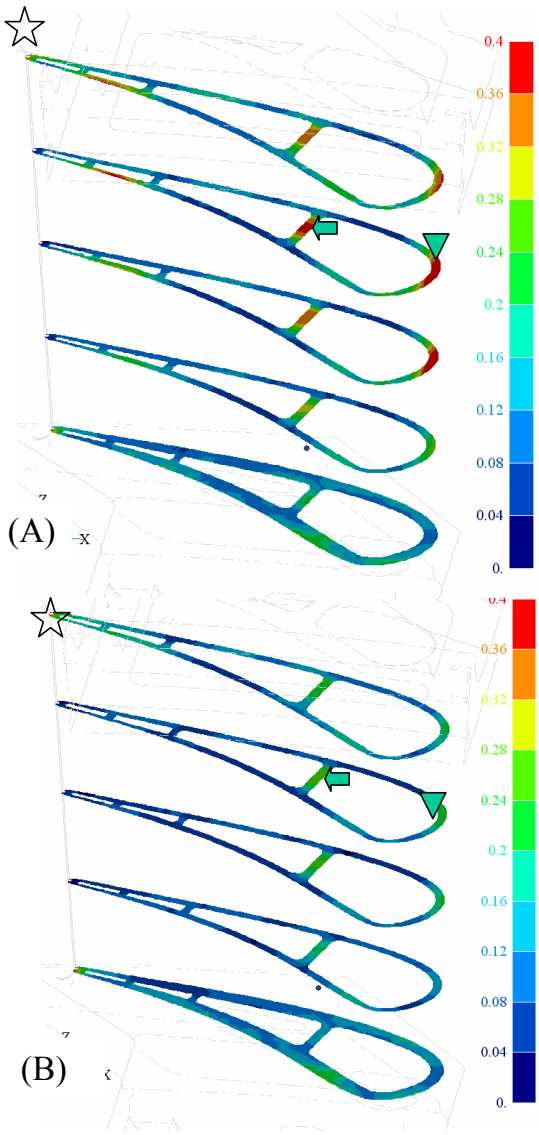

Fig. 9 Proof Ratio for TMS-75superalloys. (A) convection, (B) film cooling.

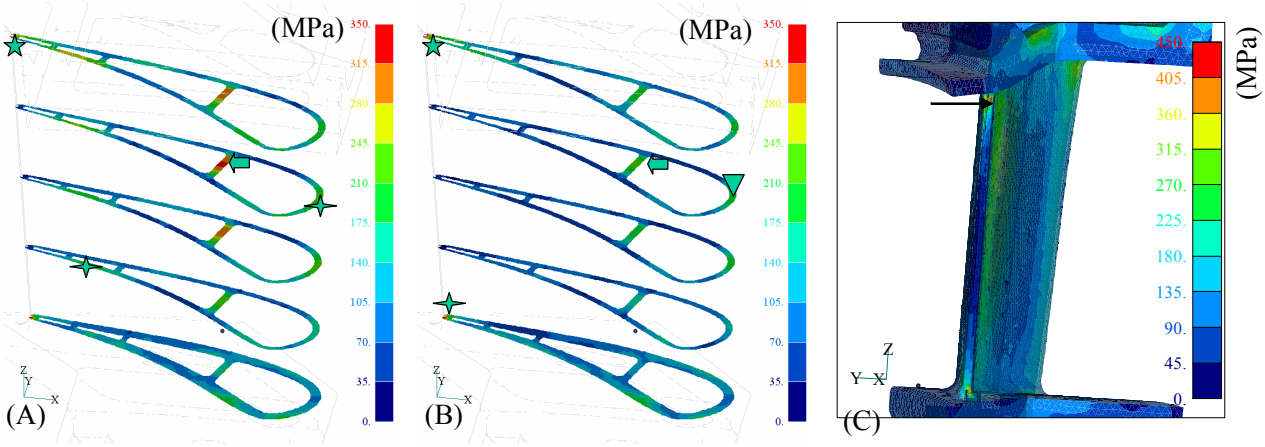

Fig. 8 Von Mises stress of TMS-75 superalloys, (A) convection, (B) film cooling, (C) contour picture of (A) as ☆

In order to have a detail view of proof ratio distribution, we virtually divide the vane into 5 parts (Height 90%, 70%, 50%, 30%, 10%) on the Z direction. Fig. 10 shows the proof ratio distribution of nodes in 5 parts on the pressure and suction surface.

For both convection case and film cooling case, at Height 90%, there are many nodes with high proof ratios. In the case of convection, the proof ratios are larger at the central part Height 70% and 50% (Fig. 10 (A)). In case of film cooling, the proof ratio of whole turbine vanes goes down; especially the proof ratios of the central parts go down significantly (Fig. 10 (B)). It is thought that the film cooling contributes more to central parts than the top and bottom parts. Therefore, thermal stress of the central parts is improved greatly. If the film cooling can extend to the top and bottom parts, lower and uniformly distributed thermal stress can be obtained.

Table 2 shows the average, minimum, maximum and standard deviation of proof ratio of the whole pressure and suction. The maximum proof ratio (Film cooling) is 0.58. But with the film cooling, the temperature, Average and standard deviation of thermal stress for turbine vanes go down. It is supposed that film cooling can extend the operational life of the turbine vanes.

Table 2 Statistical characters for proof Ratio

Parameters	Aver.	Min	Max	SD
Convection	0.14	0.02	55.1	0.07
Film cooling	0.10	0.01	58.2	0.05

CONCLUSION

In order to establish the process of structural strength analysis of TIT 1700 ℃ level virtual turbine vanes and blades, the interface of TIT 1400℃ level turbine vanes has been constructed. By utilizing the interface, thermal stress analysis and evaluation has been performed. The results obtained in the present work are:

(1) The interpolate process of three dimensions can be disassembled into two steps, selection of that interpolation plane and interpolation in two-dimensional plane. Validity of the constructed interface was verified.

(2) The maximum Von Mises stress is situated in the fillet between the trailing edge of pressure side and the outer sidewall of vane.This may due to the small radius in the relevant region in which stress concentration is easy to take place.

(3) The visualization method introduced in the present work was very effective for the evaluation of characteristics of thermal stress.

ACKNOWLEDGEMENTS

This research is a part of High-temperature material 21 project. We are grateful to the project leader Hiroshi Harada for many valuable comments on the manuscript and Tadaharu Yokogawa, Yoshitaka Fukuyama, Masahiro Matsushita and Toshio Nishizawa for supplying the experiment data.

REFERENCES

Miyazaki, N. and Shiozaki, Y., 1996, Calculation of mechanical properties of solids using molecular dynamics method, *JSME International Journal*, Vol.39, pp. 606-611.

Yoshida T., Harada H., Fukuyama Y., Ogawa A., Nozaki O., Nishizawa T., Matsushita M. and F. Zhou, 2001, Virtual Turbine: Its State of the Art and Advanced Works in the Project, *2nd International Symposium of High Temperature Materials 21*. P.64-65

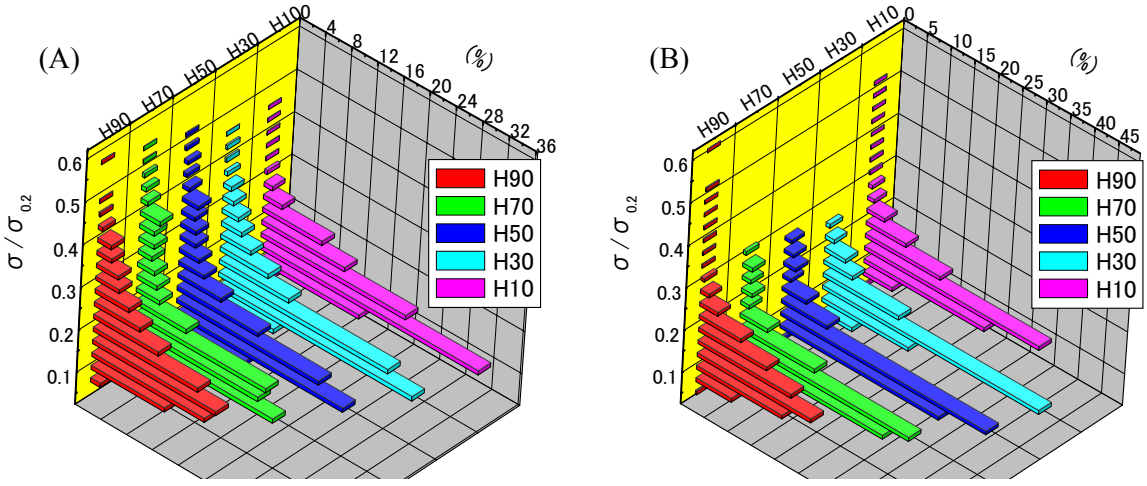

Fig. 10 Frequency distribution for proof ratio, (A) convection, (B) film cooling.